Experimental Neurology 313 (2019) 49–59

Contents lists available at ScienceDirect

Experimental Neurology

journal homepage: www.elsevier.com/locate/yexnr

Research Paper

Oncostatin M-induced upregulation of SDF-1 improves Bone marrow stromal cell migration in a rat middle cerebral artery occlusion stroke model

Jianbang Han[1], Zhiming Feng[1], Yu Xie, Feng Li, Bingke Lv, Tian Hua, Zhongfei Zhang, Chengmei Sun, Dazhuang Su, Qian Ouyang, Yingqian Cai, Yuxi Zou, Yanping Tang, Haitao Sun, Xiaodan Jiang*

Department of Neurosurgery, Zhujiang Hospital, Southern Medical University, The National Key Clinical Specialty, The Engineering Technology Research Center of Education Ministry of China, Guangdong Provincial Key Laboratory on Brain Function Repair and Regeneration, Guangzhou, China

ARTICLE INFO

Keywords:
Oncostatin M
Bone marrow-derived mesenchymal stem cells
Astrocytes
SDF-1
MCAO stroke

ABSTRACT

Bone marrow-derived mesenchymal stem cells (BMSCs) exhibit potential regenerative effects on the injured brain. However, these effects are constrained by their limited ability to migrate to the injured site. Oncostatin M (OSM) has been shown to affect the proliferation and migration of mesenchymal stem cells. Therefore, in the present study, we explored whether OSM improves BMSC migration and secretion of growth factors and cytokines in a rat middle cerebral artery occlusion (MCAO) stroke model. The effect of OSM on the proliferation and apoptosis of rat BMSCs was first assessed in vitro, and the gene and secretion levels of factors related to cell nutrition and migration, such as SDF-1 and VEGF, were detected. To further explore underlying pathways triggered by OSM, BMSCs were treated with OSM in the presence or absence of inhibitors of the STAT3 and ERK pathways. Effects of OSM on SDF-1 expression in astrocytes and BMSC migration were also evaluated. In the rat MCAO model, OSM secretion levels were detected in the brain for up to 72 h after model establishment. Ventricle injection of OSM alone or OSM combined with caudal vein graft of BMSCs was then performed in MCAO stroke rats. After 72 h, production of SDF-1 and grafted BMSCs was detected in the lesion areas of the brain, and the nerve function score was evaluated. We found that the production of OSM continually increased in the brains of MCAO rats from 12 h to 72 h. OSM significantly upregulated SDF-1 in BMSCs via the STAT3 and ERK pathways and significantly promoted the expression of VEGF and MMP-2. OSM also promoted the secretion of SDF-1 in astrocytes through the STAT3 and ERK pathways to in turn enhance BMSC migration. Combination treatment with OSM and BMSCs in MCAO rats increased the migration efficiency of BMSCs in the brain, which significantly improved neurofunctional recovery while reducing the expression of inflammatory mediators and promoting the secretion of nutrition factors. Overall, these results show that OSM is highly expressed in the brains of MCAO stroke rats and can upregulate SDF-1 to promote BMSC migration. Thus, combination treatment with OSM and BMSCs improves the graft efficiency of BMSCs and neurofunctional recovery.

1. Introduction

Bone marrow-derived mesenchymal stem cells (BMSCs) exhibit therapeutic potential to have a regenerative effect when transplanted directly into the injured brain (Lv et al., 2016). The main therapeutic mechanisms of BMSCs include their anti-inflammatory and immunomodulatory properties, induction of the expression of growth factors and cytokines, vascular effects, and promotion of remyelination (Caplan and Correa, 2011; Caplan and Dennis, 2006). However, some studies have demonstrated the low migration efficiency of BMSCs (Keimpema et al., 2009; Yang et al., 2011), resulting in the failure of some phase III clinical trials (Ankrum and Karp, 2010).

Stromal cell-derived factor-1 (SDF-1) and its receptor CXC motif receptor 4 (CXCR4) play an important role in regulating the migration of BMSCs (Sohni and Verfaillie, 2013). In cerebral ischemia, SDF-1 is secreted by astrocytes around the infarcted region and attracts stem

Abbreviations: BMSCs, bone marrow-derived mesenchymal stem cells; CXCR4, chemokine (C-X-C motif) receptor 4; IL, interleukin; MCAO, middle cerebral artery occlusion; OSM, oncostatin M; SDF-1, stromal-derived cell factor-1; mNSS, modified neurological severity score; VEGF, vascular endothelial growth factor

* Corresponding author.
E-mail address: jiangxiao_dan@163.com (X. Jiang).

[1] These authors have contributed equally to this work

https://doi.org/10.1016/j.expneurol.2018.09.005
Received 25 January 2018; Received in revised form 3 September 2018; Accepted 7 September 2018
Available online 11 September 2018
0014-4886/

cells (Imitola et al., 2004). CXCR4 is a chemokine receptor specific for SDF-1; pretreatment of mesenchymal stem cells (MSCs) with its antagonist inhibits MSC homing into the infarcted area (Wang et al., 2008). Indeed, modification of the SDF-1/CXCR4 axis with various drugs or cytokines such as DETA-NONOate (Cui et al., 2007), VPA (Tsai et al., 2011), PEG2 (Hoggatt et al., 2009), and some biomaterials (Huang et al., 2016; Shi et al., 2016), has been found to enhance the migration rates of implanted stem cells. In addition,inflammatory cytokines play important roles in the pathogenesis of stroke. For example, interleukin (IL)-1β-knockout mice exhibit markedly reduced brain damage upon middle cerebral artery occlusion (MCAO) (Boutin et al., 2001), while increased brain damage occurs when IL-1β is administered to rats (Yamasaki et al., 1995). IL-6 leads to an excessive inflammatory response, which may increase injury due to stroke (Jin et al., 2013). By contrast, VEGF is a trophic factor that has acute neuroprotective, neurogenic, and angiogenic effects in post-ischemic brain repair (Greenberg and Jin, 2013).

Oncostatin M (OSM) belongs to the IL-6 family of cytokines, which also includes ciliary neurotrophic factor, leukemia inhibitory factor, IL-11, cardiotrophin-1, and cardiotrophin-like cytokine (Chen and Benveniste, 2004). OSM exerts many benefits effects in central nervous system diseases, such as demyelinating disease (Glezer and Rivest, 2010), spinal cord injury (Slaets et al., 2014), and ischemic stroke (Guo et al., 2015). The main function of OSM is regulation of the astrocytes and microglia (Baker et al., 2008), maintaining balance in the context of inflammation and neuroprotection, and enhancing oligodendrocyte precursor cell activity at demyelinated sites (Janssens et al., 2015; Beatus et al., 2011; Glezer and Rivest, 2010). Moreover, OSM enhances the secretion of growth factors and cytokines by BMSCs, and OSM preconditioning was shown to affect the proliferation and migration of MSCs (Lan et al., 2017; Albiero et al., 2015).

Therefore, in this study, we explored whether OSM promotes BMSC migration via SDF-1 along with other trophic and inflammatory factors. We further examined the potential mechanism underlying the effects of OSM treatment in increasing the levels of migration-related factors and the secretion of cytokines to ultimately promote the migration of BMSCs into the ischemic brain. For this, we evaluated the effects of OSM on BMSC proliferation, migration, and protein expression in vitro. We further evaluated the potential therapeutic effects of OSM by monitoring the migration efficiency of BMSCs alone and in combination with OSM injected into rats subjected to MCAO.

2. Materials and methods

2.1. Animals

Sprague-Dawley (SD) rats were purchased from the Laboratory Animal Center of Southern Medical University. The rats were maintained under laboratory conditions with free access to a standard diet and sterile water under a controlled temperature (24 °C). All animal procedures were performed in accordance with the guidelines of our institute and were approved by the Animal Ethics Committee of Southern Medical University.

2.2. MCAO model establishment

SD rats weighing 250–300 g (age 10–12 weeks) were allowed free access to water but were fasted for 12 h to standardize glycemic state. Anesthesia was induced by intraperitoneal injection of pentobarbital (100 mg/kg). Body temperature was maintained at 37 ± 0.5 °C using a heating pad (RWD Life Science, Shenzhen, China). To induce MCAO in the rats, a 4-0 suture (Covidien, Mansfield, MA, USA) with a round tip and silicon coating was inserted from the left external carotid artery into the middle cerebral artery (Yang et al., 1994). The success of the surgery was verified by detection of surface cerebral blood flow using a laser Doppler flowmeter (Moor LAB, Moor Instruments, Devon, UK). At 2 h after insertion of the suture, the rats were re-anesthetized, and the suture was withdrawn to perform reperfusion. The rats in the control group underwent a sham operation without suture insertion.

After MCAO, the rats were randomly divided into three groups (n = 5 rats per group): sham, same operation without suture insertion; MCAO only; and MCAO + OSM injection via the tail vein.

2.3. Cell isolation and culture

BMSCs were isolated from the bilateral femurs and tibias of SD rats as previously described (Islam et al., 2012). The cells were collected by centrifugation at 1000 rpm for 5 min, suspended in Dulbecco's modified Eagle medium (DMEM)/F-12 supplemented with 10% fetal bovine serum (FBS) and penicillin/streptomycin (100 U/ml, Gibco, Franklin Lakes, NJ, USA), and grown at 37 °C in a humidified 5% CO_2 atmosphere. After 72 h, the non-adherent cells were discarded, and fresh culture medium was added. The culture medium was changed every 3 days, and the cells were passaged at approximately 80% confluence.

Astrocytes were isolated from the brains of newborn (within 24 h of birth) SD rats as previously described (Hayakawa et al., 2016). The cerebral cortex was collected under sterile conditions and washed in cold phosphate-buffered saline (PBS). The meninx and blood vessels on the surface were carefully removed, and the remaining cerebral cortex was cut into cubes in serum-free DMEM before digestion in 0.05% trypsin (Gibco) and DNase I for 10 min at 37 °C. After digestion, the suspension was centrifuged at 1000 rpm for 5 min, and the cells were resuspended in DMEM supplemented with 10% FBS and penicillin/streptomycin (100 U/ml). The cells were then incubated at 37 °C in a humidified atmosphere under 5% CO_2; after approximately 1 week, the cells were separated into two layers: lower astrocytes and upper putative microglia. The cells were digested in 0.005% trypsin for 5 min, and then the trypsin was discarded and replaced with fresh medium.

2.4. BMSC transplantation and tracking

The rats were randomly divided into the following three groups (n = 5 rats per group) after MCAO: MCAO + DMEM, MCAO + BMSCs, and MCAO + BMSCs + OSM. The transplantation of BMSCs through caudal vein injection (3×10^6 cells in 1 ml DMEM) was performed 2 h after transient MCAO. The same amount of DMEM without cells was injected as the control.

To trace the internal migration of the BMSCs toward the lesion site, transfection was carried out using a green fluorescent protein (GFP) lentivirus (Obio Technology, Shanghai, China), in accordance with the manufacturer's instructions. The number of GFP-positive BMSCs was counted under a fluorescence microscope. In addition, total protein was collected from each group to measure the expression of IL-1β, IL-6, and VEGF by western blotting.

2.5. Effect of OSM on the proliferation of BMSCs in vitro

The viability of the BMSCs was evaluated after treatment with OSM using the CCK-8 Cell Proliferation Assay Kit (ATCC, Manassas, VA, USA) according to the manufacturer's instructions. In brief, BMSCs (1×10^4 cells) were seeded in a 96-well plate until adherence and then treated with OSM for various durations. CCK-8 reagent was then added to the plates, cells were incubated in the dark at room temperature for 2 h, and the optical density was detected at 450 nm using the iMark microplate reader (Bio-Rad, Hercules, CA, USA).

Proliferation was also determined using the 5-ethynyl-2′-deoxyuridine (EdU) assay with the EdU labeling/detection kit (Ribobio, Guangzhou, China) according to the manufacturer's instructions. In brief, 50 μmol EdU labeling medium was added to the cell culture and incubated for 4 h at 37 °C under 5% CO_2. The cells were then fixed with 4% paraformaldehyde in PBS for 15 min and permeabilized with 0.5% Triton-X-100 for 20 min, followed by incubation with glycine for 5 min.

After washing with PBS, the cells were stained with anti-EdU working solution at room temperature for 30 min. Following a wash with 0.5% Triton X-100 in PBS, the cells were incubated with 5 μg/ml Hoechst 33342 dye at room temperature for 30 min, followed by observation under a confocal laser-scanning microscope (TCS SP2, Leica Microsystems, Germany). The percentage of EdU-positive cells was calculated from four random fields in each well. Each experiment was repeated three times.

2.6. Apoptosis assay

Quantification of apoptosis was performed using an Annexin V-FITC Apoptosis Detection Kit (BD Biosciences, San Jose, CA, USA) according to the manufacturer's recommendations. A total of 1×10^4 cells were resuspended in 100 μl annexin binding buffer by adding 10 μl annexin V-FITC and 5 μl propidium iodide. After 30 min of incubation in the dark, the cells were analyzed by flow cytometry on a Becton-Dickinson FACS flow cytometer (BD Biosciences, Franklin Lakes, NJ, USA) within the first hour. This experiment was repeated three times.

2.7. Enzyme-linked immunosorbent assay (ELISA)

BMSCs were treated with or without OSM in the presence or absence of AG490 or U0126. The levels of SDF-1 were measured using DuoSet ELISA kits (Elabscience Biotechnology Co., Ltd., Shanghai, China) in accordance with the manufacturer's instructions. The samples were centrifuged at 1800 ×*g* at 4 °C for 10 min. All analyses were carried out in duplicate, using the proposed substrates, buffers, and diluents. Each experiment was repeated four times, and the final outcomes were pooled as the average concentration of SDF-1.

2.8. Transwell migration assay

The effect of OSM on the migration ability of BMSCs was assessed using Transwell chambers, which were 6.5 mm in diameter, with 8-μm nitrocellulose pore filters (Amersham Biosciences, Piscataway, NJ, USA). In the chemotaxis group, 200 μl of serum-free culture medium containing 1×10^5 BMSCs was added to the upper chambers, and 800 μl DMEM containing 1×10^6 BMSCs, 50 ng/ml of OSM, and 2% FBS was added to the lower chambers. In the chemotaxis inhibition group, 200 μl of serum-free culture medium containing 1×10^5 BMSCs was added to the upper chambers, and 800 μl DMEM containing 1×10^6 BMSCs, which had been co-cultured with 10 μg/ml of the STAT3 inhibitor AG490 (S1143) or 10 μg/ml of the ERK inhibitor U0126 (S1102) at 37 °C for 2 h, was added to the lower chambers. In the control group, 200 μl of serum-free culture medium containing 1×10^5 BMSCs was added to the upper chambers, and 800 μl of DMEM containing 1×10^6 BMSCs was added to the lower chambers.

The effect of OSM on the chemotaxis ability of astrocytes was also evaluated in a similar manner. In the chemotaxis group, 200 μl of serum-free culture medium containing 1×10^5 BMSCs was added to the upper chambers, and 800 μl of DMEM containing 1×10^6 astrocytes, 50 ng/ml of OSM, and 2% FBS was added to the lower chambers. In the chemotaxis inhibition group, 200 μl of serum-free culture medium containing 1×10^5 BMSCs was added to the upper chambers, and 800 μl of DMEM containing 1×10^6 astrocytes, which had been co-cultured with 5 μg/ml anti-SDF-1 (ab25117, Abcam, Cambridge, UK) at 37 °C for 2 h, was added to the lower chambers. In the control group, 200 μl of serum-free culture medium containing 1×10^5 BMSCs was added to the upper chambers, and 800 μl of DMEM containing 1×10^6 astrocytes was added to the lower chambers.

Following incubation for 8 h, the non-migrated cells in the upper chamber were cleared, and the membranes were fixed with 4% paraformaldehyde for 30 min. The migrated cells were stained with 5% crystal violet dye solution (Saichuang Technology, Wuhan, China) for 20 min, washed with PBS, and then photographed under a microscope (Eclipse Ti-E/U/S, Nikon, Tokyo, Japan). The average number of migrated BMSCs was determined from five randomly chosen fields by three blinded observers. Each experiment was repeated at least three times.

2.9. Immunohistochemistry and Immunofluorescence assays

At 72 h after MCAO, the rats were anesthetized and transcardially perfused with 100 ml cold PBS and 100 ml of 4% paraformaldehyde in 0.1 M PBS. The brains were then removed, post-fixed, and paraffin-embedded, and consecutive coronal sections were cut at 5-μm intervals from −2.0 mm of the bregma to −7.0 mm of the bregma to collect the entire lesioned cortex. For immunohistochemistry, slides with brain sections were deparaffinized and boiled in 10 mM citrate buffer (pH 6.0) in a microwave to expose the antigens before being blocked with 10% normal goat serum. The slides were incubated with a primary antibody against SDF-1 (ab25117, Abcam) at 4 °C overnight, followed by incubation with with an avidin-biotin-peroxidase system (Boster); negative controls were stained with the secondary antibody only. Finally, the slides were stained with diaminobenzidine, and the nucleus was counterstained with hematoxylin.

To identify SDF1 and GFAP expression in brain tissues or astrocytes, immunofluorescence staining was used as described previously (Cui et al., 2007). Each specimen was first treated with primary anti-SDF1 and anti-GFAP [#3670, Cell Signaling Technology (CST), Danvers, MA, USA] antibodies, then fluorescent Alexa 594-conjugated (A0453) antibody was used for SDF-1, while fluorescent Alexa 488-conjugated antibody (A0428) was used for GFAP. Immunofluorescent images were acquired using a model TCS SP2 confocal laser-scanning microscope (Leica Microsystems).

2.10. Real-time polymerase chain reaction (PCR)

Total RNA was collected from BMSCs, astrocytes, and brain tissues using column purification (Qiagen, Gaithersburg, MD) as described previously (Tang et al., 2014). First-strand cDNA was generated with random primers using iScript cDNA synthesis kits. Quantitative PCR was performed using the SYBR Green real-time PCR method(TaKaRa) on an LC480 PCR instrument (LightCycler® 480 II)using three-stage program parameters provided by the manufacturer. Each sample was tested in triplicate, and analysis was performed according to the ΔΔCt method. The primers used for real-time PCR are shown in Table 1.

2.11. Western blotting

Total protein was isolated from BMSCs, astrocytes, and brain tissues, and total protein concentrations were measured with the BCA Protein Assay Kit (ThermoFisher Scientific, Waltham, MA, USA). The protein samples (30 mg) were separated by sodium dodecyl sulfate–-polyacrylamide gel electrophoresis and then transferred onto a polyvinylidene fluoride membrane (Millipore Corporation, Billerica, MA, USA). The membranes were blocked with 5% non-fat milk and 0.05% Tween-20 at room temperature for 2 h, followed by overnight incubation at 4 °C with rabbit anti-OSM (ab133748, Abcam), p65 (#8242, CST), p-p65 (#3033, CST), ERK (#4695, CST), p-ERK (#4370, CST), STAT3 (ab68153, Abcam), and p-STAT3 (ab76315, Abcam) antibodies (all diluted 1:1000), as well as rabbit anti-SDF-1 (diluted 1:500), VEGF (19003–1-AP, Proteintech, Rosemont, IL, USA), IL-6 (ab9324, Abcam), and IL-1β (#12703, CST) antibodies. The membranes were then washed three times and incubated with horseradish peroxidase-conjugated anti-mouse or anti-rabbit secondary antibodies at a dilution of 1:5000 for 1 h at room temperature. Finally, an enhanced chemiluminescence detection reagent (Pierce, Rockford, IL, USA) was used to develop the protein bands, which were quantified by Quantity one 1-D analysis software (Version 4.4, Bio-Rad) and normalized to the corresponding GADPH internal control (60004-1-Ig, Proteintech). All immunoblots were

Table 1
Real-time PCR primers.

Gene	Forward primer (5′–3′)	Reverse primer (5′–3′)
GAPDH	AGAACATCATCCCTGCATCC	CACATTGGGGGTAGGAACAC
SDF1	AGCCTTAAACAAGAGGCTCAAG	GTTTGGGCGGAACAACAGAC
VEGF	TTCGTCCAACTTCTGGGCTC	GCTTTCTGCTCCCCTTCTGT
CXCR4	GGCTGTAGAGCGATGTTTGC	GTAGAGGTTGACAGTGTA
CXCR7	CCGCGAGGTCACTTGGTT	CAGTGTGTGTCGTAGCCTGT
MMP9	AATCTCTTCTAGAGACTGGGA AGGAG	AGCTGATTGACTAAAGTAGCT GGA
MMP2	AGCAAGTAGACGCTGCCTTT	CAGCACCTTTCTTTGGGCAC

GAPDH: glyceraldehyde-3-phosphate dehydrogenase.
SDF1: stromal-derived cell factor-1.
VEGF: vascular endothelial growth factor.
CXCR4: chemokine (C-X-C motif) receptor 4.
CXCR7: chemokine (C-X-C motif) receptor 7.
MMP9: matrix metalloprotein 9.
MMP2: matrix metalloprotein 7.

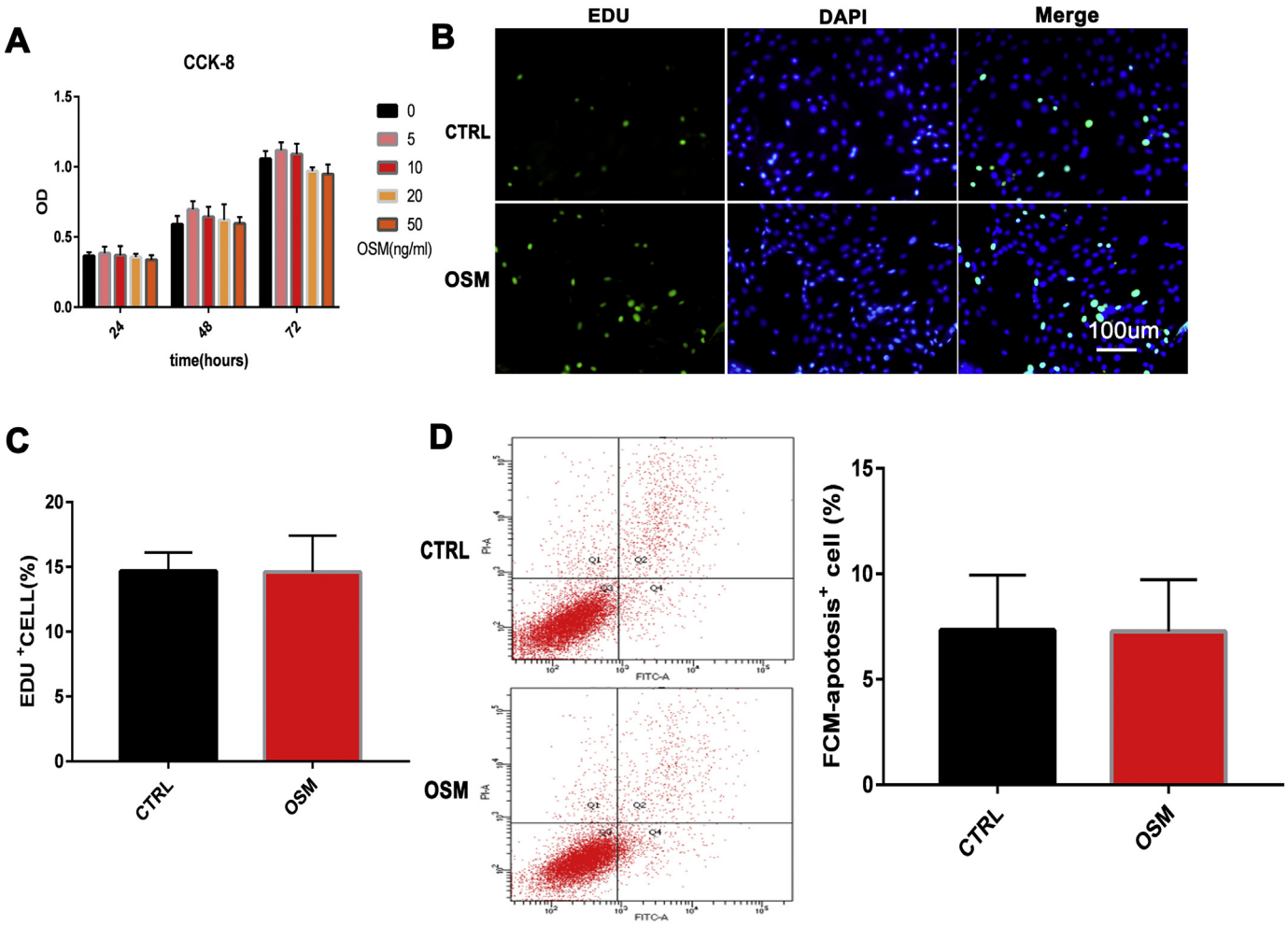

Fig. 1. OSM has no effect on the proliferation or apoptosis of BMSCs. BMSCs were treated with or without OSM,. No impact on the BMSCs proliferation (A–C) and apoptosis (D) were measured by CCK8 and EdU assays(The Green/EDU$^+$ cells is indicate in the period of proliferation rate (B).;proliferation efficiency = the number of green cells/the number of blue cells × *100% (C).), Apoptosis was measured by and Annexin V-FITC/PI staining with flow cytometry assays (D). Scale bar: 100 μm. The data are plotted as the means ± SD. *P > 0.05, n = 3. (For interpretation of the references to colour in this figure legend, the reader is referred to the web version of this article.)

repeated at least three times independently, and relative protein expression is expressed as a ratio to the internal control.

2.12. Therapeutic efficiency

The therapeutic effects of BMSCs with and without OSM in the MCAO rats were assessed using the modified neurological severity score (mNSS) and foot-fault tests conducted by a blinded investigator before MCAO and at 7 days after MCAO, as previously described (Lv et al., 2017). The mNSS is a composite of the motor (muscle status and abnormal movement), sensory (visual, tactile, and proprioceptive), and reflex tests. The rats were evaluated by several tests, such as raising the

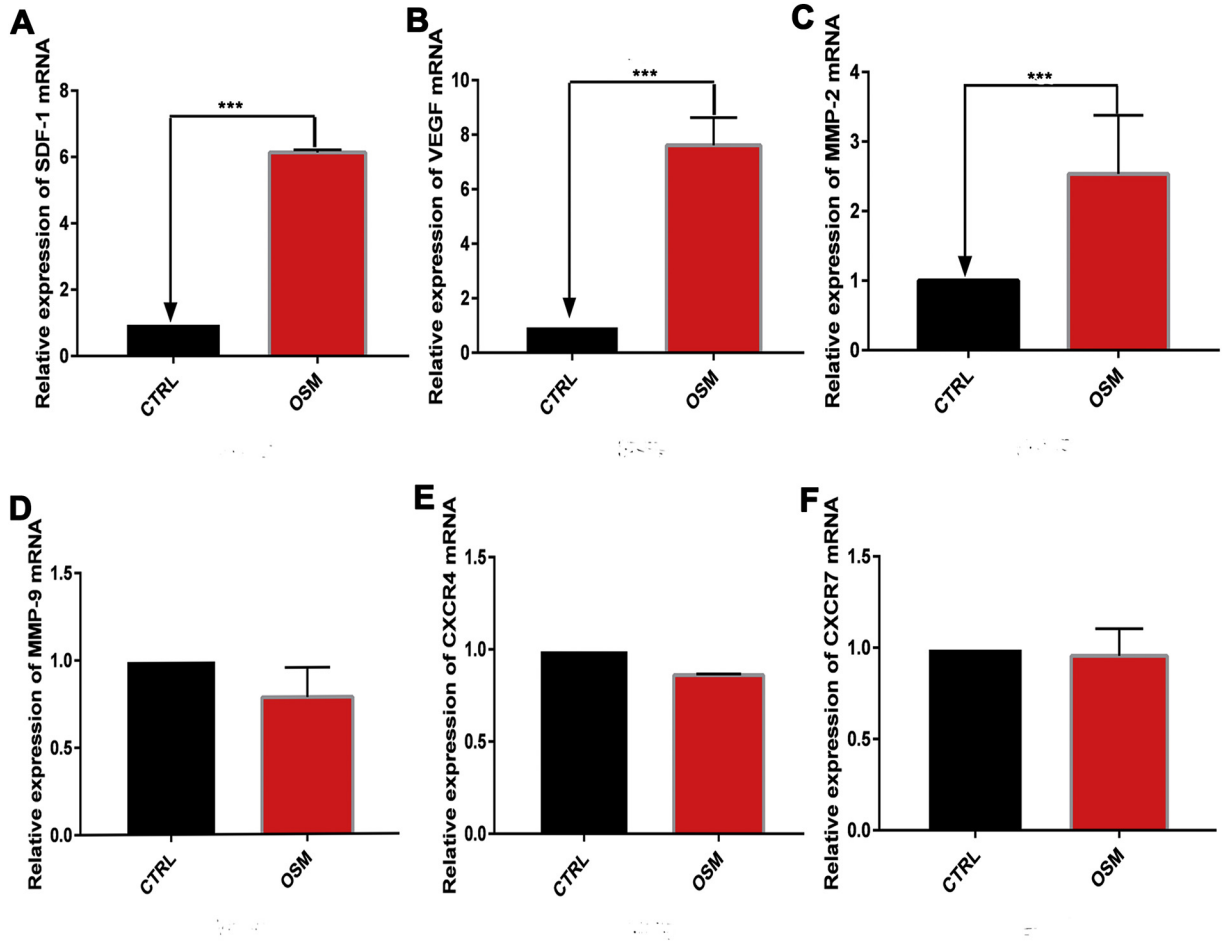

Fig. 2. OSM alters the expression of nutrition- and migration-related factors of in BMSCs. BMSCs were treated with or without OSM. The mRNA levels of (A) *SDF-1* (A), (B) *VEGF*(B) CXCR4 (C), CXCR7 (D), MMP9 (E), and (F) MMP-2 (F) were upregulated, but no significant difference was found in mRNA levels of (C) CXCR4, (D) CXCR7, and (E) MMP-9. The data are plotted as the means ± SD. ***P < 0.001, n = 3.

rat by the tail, placing the rat on the floor, and beam balance walking, then all test scores were compiled into the mNSS score. The neurological function was graded on a scale of 0–18 (normal score 0, maximal deficit score 18) (Piao et al., 2018). The infarct areas of different experimental groups (5 sections/animal) were determined by photomicrographs obtained from cresyl violet-stained sections (Franco et al., 2012). Experiments were repeated five times.

2.13. Statistical analysis

Data are presented as the mean ± standard deviation of three to five independent experiments. Data were analyzed with SPSS 20 software (SPSS Inc., Chicago, IL, USA). Differences between the two groups were evaluated by Student's *t*-test. One-way analysis of variance was used to analyze the differences of three or more groups. $P < 0.05$ was considered to indicate statistical significance.

3. Results

3.1. Effect of OSM on proliferation, apoptosis, and expression of nutrition- and migration-related factors in BMSCs

To evaluate the effect of OSM on the proliferation and apoptosis of BMSCs in vitro, CCK8/EdU assays and annexin V-FITC/PI staining with flow cytometry were performed, respectively. As shown in Fig. 1A, treatment with different concentrations of OSM had no impact on BMSC proliferation over time. Further, there was no significant difference in apoptosis rates between the OSM-treated group and blank control group (Fig. 1B; $P > 0.05$).

The mRNA levels of SDF-1, VEGF, and MMP-2 were significantly higher in the OSM-treated BMSCs than in control BMSCs ($P < 0.01$), whereas there was no significant difference in the expression of CXCR4, CXCR7, and MMP-9 between the two groups (Fig. 2; $P > 0.05$).

3.2. OSM enhances SDF-1 expression through the STAT3 and ERK pathways to promote the migration of BMSCs

Next, we detected whether OSM influenced the migration of BMSCs by upregulating the expression of SDF-1 through the STAT3 and ERK pathways. After BMSCs were stimulated by OSM, the STAT3 and ERK pathways were activated (Fig. 3A–C). Moreover, OSM upregulated the secretion of SDF-1 in BMSCs, which was inhibited by the STAT3 inhibitor AG490 and the ERK inhibitor U0126 (Fig. 3D, E). Finally, Transwell assays showed that the number of migrating BMSCs was significantly increased after OSM stimulation and reduced upon treatment with the inhibitor AG490 or U0126 (Fig. 3F).

3.3. OSM upregulates SDF-1 expression via STAT3 and ERK pathways in astrocytes to promote the migration of BMSCs

We also evaluated the effect of OSM on the migration and expression levels of astrocytes. As shown in Fig. 4, OSM treatment significantly upregulated the production of chemokines such as MCP-1, CXCL-1, and SDF-1. Specifically, the mRNA expression levels of MCP-1,

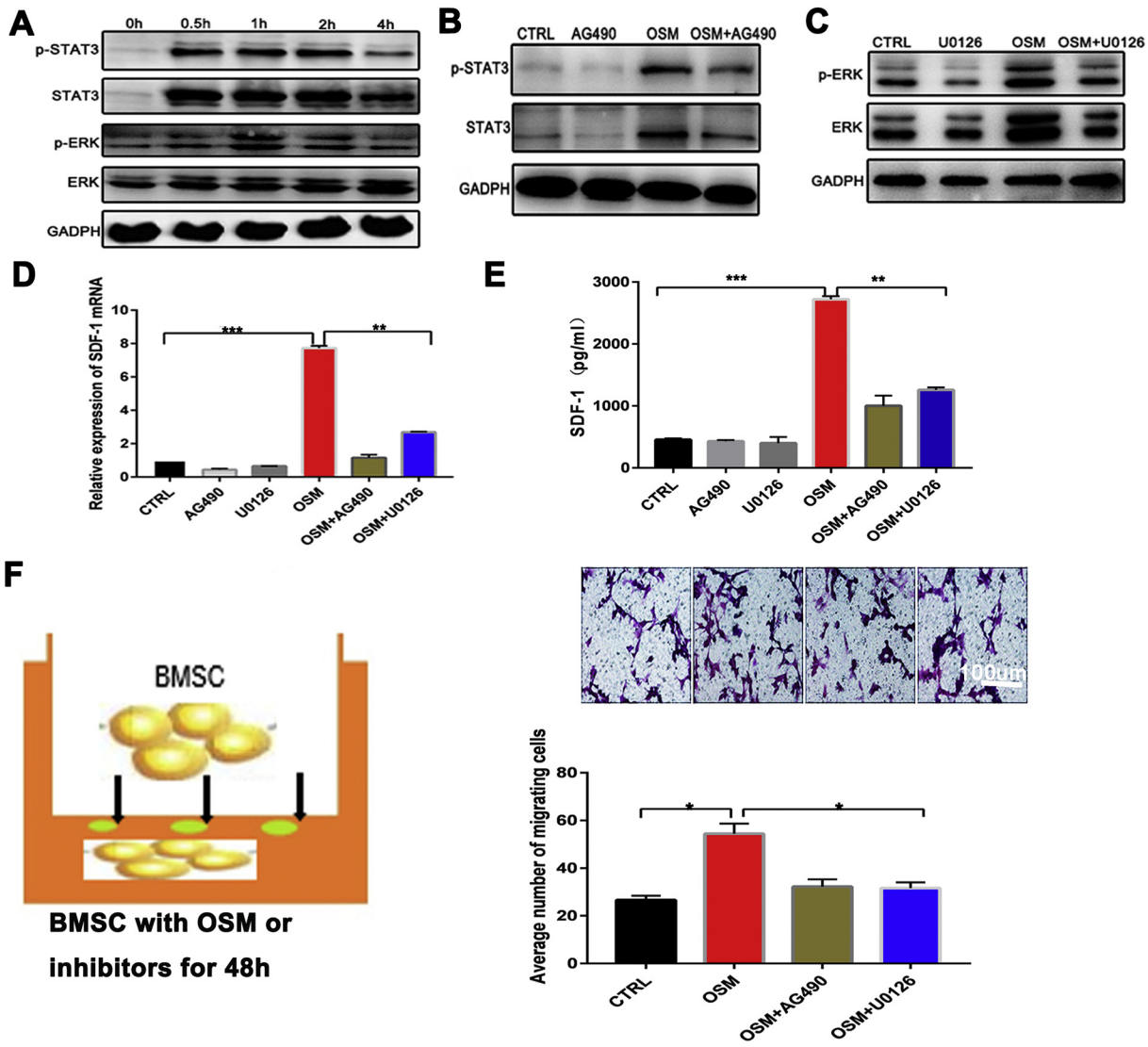

Fig. 3. OSM enhances the expression of SDF-1 through the STAT3 and ERK pathways to promote the migration of BMSCs. BMSCs were treated with or without OSM in the presence or absence of AG490 or U0126. The STAT3 and ERK pathways were activated by OSM and inhibited by AG490 or U0126, respectively (A–C). While SDF-1 expression was also upregulated by OSM and inhibited by AG490 or U0126 (D-E). Average number of migrated BMSCs was increased by OSM and reduced by AG490 or U0126 (F). Scale bar: 100 μm. The data are plotted as the means ± SD. ***P < 0.001, **P < 0.01, *P < 0.05, n = 4.

CXCL-1, and SDF-1 in the OSM treatment group were 3.74-fold, 3.47-fold, and 2.92-fold higher than those in the control group, respectively (all P < 0.01). In addition, levels of proteins in the STAT3 and ERK pathways significantly increased upon OSM stimulation. Moreover, the fluorescence intensity of SDF-1 in the OSM group was significantly higher than that in the control group. Finally, OSM stimulation of astrocytes increased the number of BMSCs migrating to the lower chamber (P < 0.01); however, after blocking SDF-1 expression with anti-SDF-1, the number of migrating BMSCs was significantly reduced (P < 0.05).

3.4. OSM was highly expressed in the brains of MCAO stroke rats

Western blotting showed that protein expression levels of OSM in the brains of MCAO rats gradually increased over time. OSM expression peaked at 12 h and then remained stable thereafter until 72 h (Fig. 5; P < 0.0001).

3.5. OSM promotes SDF-1 production in the MCAO rat brain to improve the effects of BMSC treatment

To evaluate the functional outcome of OSM in BMSC treatment in MCAO rats, the production of SDF-1 was detected by western blotting, immunohistochemistry, and immunofluorescence. As shown in Fig. 6A–C, the expression of SDF-1 was significantly higher in the OSM + BMSC treatment group than in MCAO model group. Double immunofluorescence histochemistry also showed higher SDF-1 expression in the OSM + BMSC treatment group (Fig. 6D). More importantly, OSM increased the number of migrating BMSCs: the number of GFP-positive cells in the OSM + BMSC treatment group was significantly higher than that in the BMSC-only group (Fig. 6E, P < 0.05). Furthermore, the lesion area was significantly reduced in the OSM + BMSC treatment group (Fig. 6G, P < 0.05), while the mNss score of the OSM + BMSC treatment group was significantly lower than that in the BMSC-only group (Fig. 6F, P < 0.05), indicating that the therapeutic efficiency of BMSCs was enhanced by OSM.

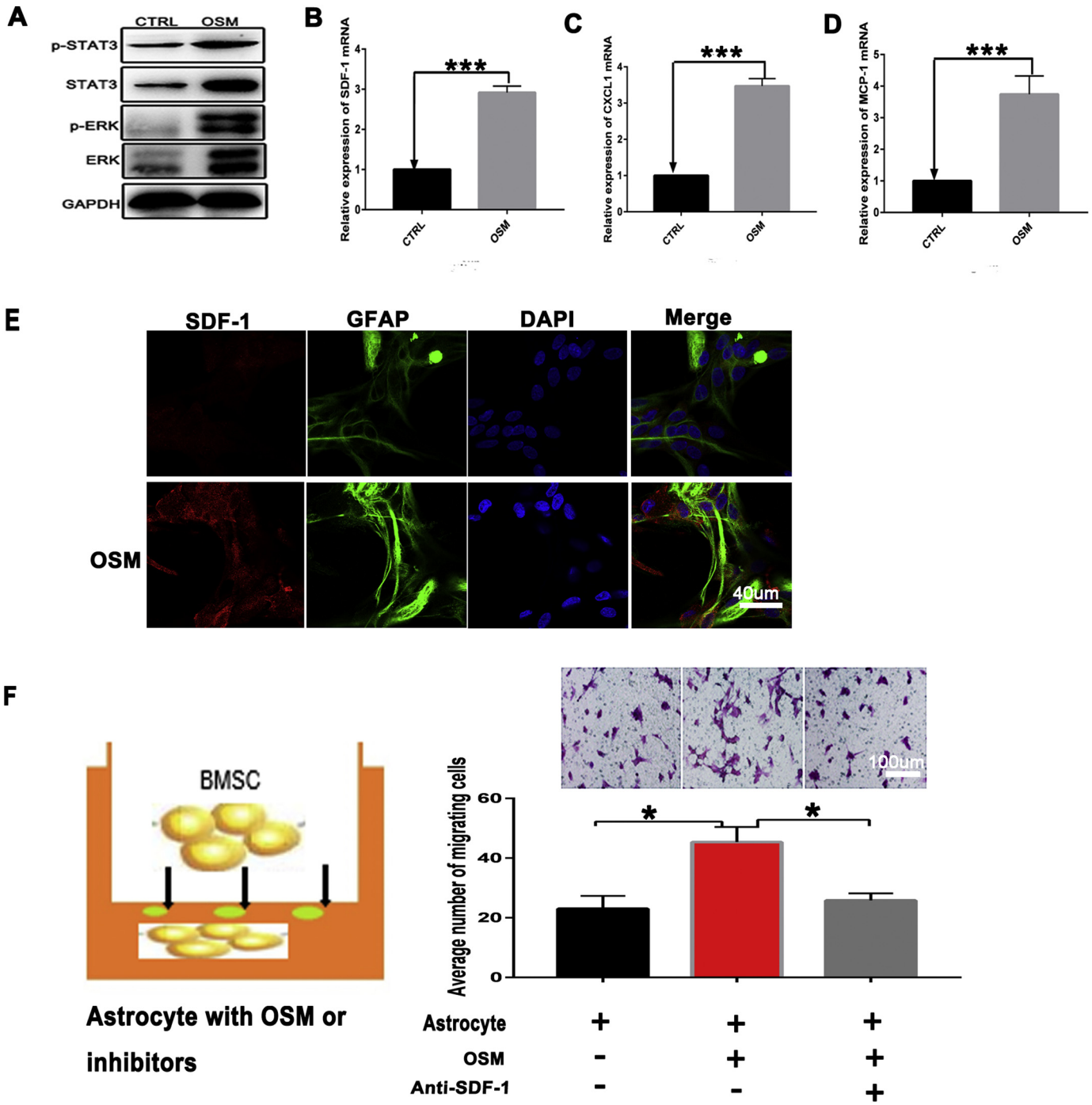

Fig. 4. OSM enhances the expression of SDF-1 in astrocytes to promote the migration of BMSCs and activated the STAT3 and ERK pathways. Astrocytes were treated with or without OSM. The protein levels of ERK, p-ERK, STAT3, and p-STAT3 in astrocytes were upregulated (A). The mRNA levels of SDF-1 (B), CXCL-1 (C), and MCP-1 (D) were upregulated by OSM. The fluorescence intensity of SDF-1 in the OSM group were increased (Scale bar: 40 μm) (E). Average number of migrated BMSCs was increased by OSM and reduced by Anti-SDF-1 (Scale bar: 100 μm) (F). The data are plotted as the means ± SD. ***P < 0.001, *P < 0.05, n = 5.

3.6. Combination OSM and BMSC treatment reduces the expression of inflammatory factors and increases the expression of trophic factors

We further explored whether OSM influenced the production of inflammatory and trophic factors when combined with BMSCs for the treatment of MCAO in rats. The western blotting results showed that protein levels of the inflammatory cytokine IL-1β were significantly lower in the OSM + BMSC treatment group than in the BMSC-only group, whereas there was no difference in the levels of IL-6 (Fig. 7A). By contrast, the expression level of VEGF was significantly higher in the OSM + BMSC treatment group than in the BMSC-only group (Fig. 7B).

4. Discussion

In this study, we demonstrated that OSM has no effect on the proliferation or apoptosis of BMSCs but increases the expression levels of SDF-1, VEGF, and MMP-2. Elevated SDF-1 production in turn enhances BMSC migration. Similarly, OSM upregulates SDF-1 expression in cultured astrocytes, which further promotes BMSC migration. These in vitro effects were further confirmed to enhance the therapeutic efficacy

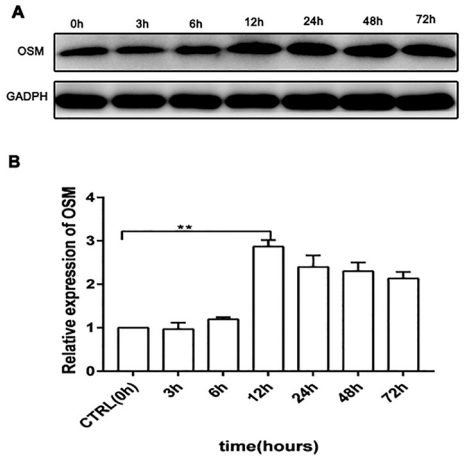

Fig. 5. Production of OSM in the brains of MCAO rats. Total protein was isolated from the cerebral cortex during the first 72 h after MCAO and measured by western blotting. Protein levels of OSM reached the maximum level, and then stabilized thereafter for 72 h. The data are plotted as the means ± SD. **P < 0.01, n = 3.

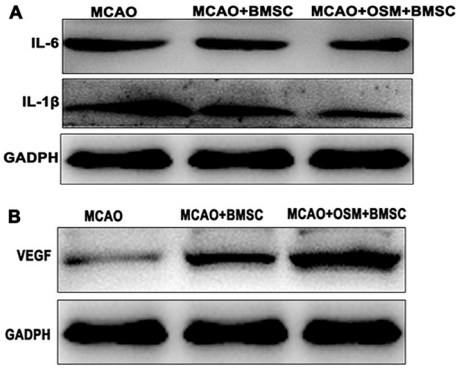

Fig. 7. Combination OSM and BMSCs treatment influences the expression of inflammatory and trophic factors. MCAO rats were treated with or without BMSCs in the presence or absence of OSM. The protein levels of IL-1β was significantly reduced in the OSM combined with BMSC treatment group, but no difference in IL-6 was found(A). The expression level of VEGF was significantly increased in the OSM combined with BMSC treatment group (B).

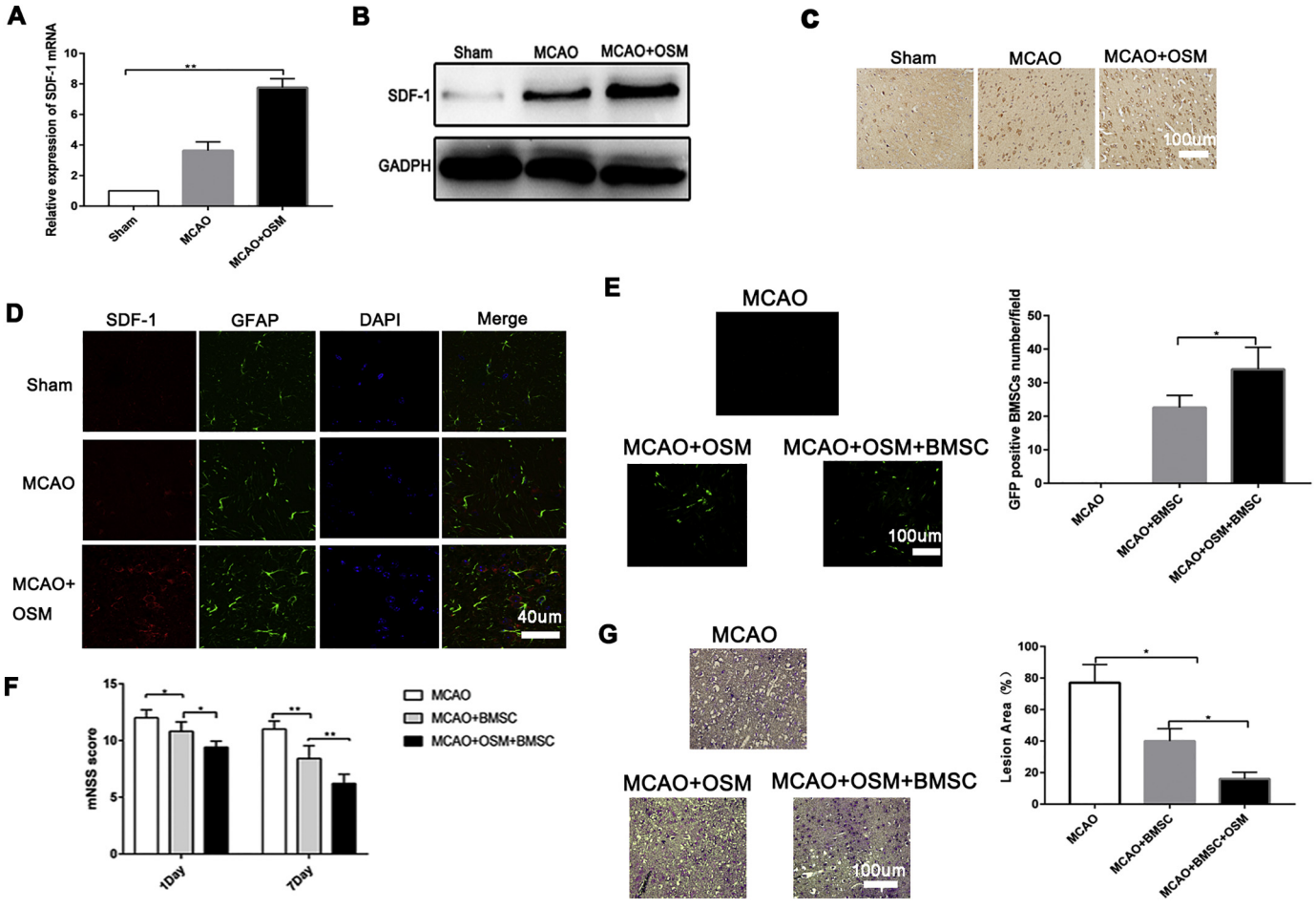

Fig. 6. OSM improves the therapeutic effect of BMSCs to in MCAO rats by promoting SDF-1 production. MCAO rats were treated with GFP-labeled BMSCs in the presence or absence of OSM. SDF-1 was significantly higher in OSM combined with BMSC treatment group than that in MCAO model group alone, which was detected by qPCR (A), western blotting (B), immunohistochemistry (Scale bar: 100 μm) (C), and double immunofluorescence histochemistry (Scale bar: 40 μm) (D). Numbers of GFP-labeled BMSCs, were significantly higher in OSM combined with BMSC treatment group, which was detected by fluorescence microscopy (Scale bar: 100 μm) (E). The mNss of the rats in each group, which as evaluated at on Day1 and Day 7 shows lower scores of OSM combined with BMSC treatment group (F). While Lesion areas was significantly reduced in OSM combined with BMSC treatment group(G) (Scale bar: 100 μm) (G). The data are plotted as the means ± SD. **P < 0.01, *P < 0.05, n = 5.

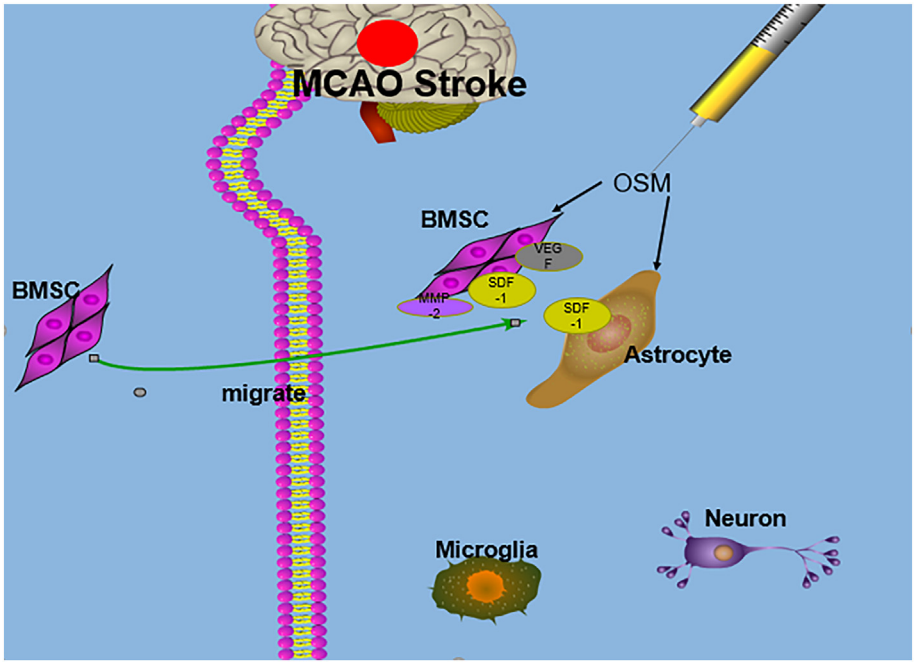

Fig. 8. Schematic diagram of the effects of OSM on BMSCs directly or through astrocytes, and the combined effects of OSM and BMSCs in the MCAO stroke model. Following stimulation with OSM, astrocytes secrete SDF-1, which induces greater numbers of BMSCs to migrate into the injured brain. Meanwhile, OSM upregulates the expression of SDF-1, VEGF, and MMP-2 in BMSCs, and the enhanced SDF-1 also promotes the migration of BMSCs into the injured brain.

of BMSCs in a rat MCAO model, in which OSM increased SDF-1 expression in the ischemic brains of MCAO rats. Treatment with a combination of OSM and BMSCs enhanced BMSC migration into the ischemic brain and improved neurobehavioral outcomes. In addition, the combination therapy further inhibited pro-inflammatory cytokine generation while promoting trophic factor secretion.

SDF-1 is an important factor in the migration of stem cells in the injured brain, and astrocytes are some of the most prominent producers of SDF-1 in the inflamed central nervous system (Blazevski et al., 2015; Luo et al., 2016). Therefore, some researchers have attempted to enhance the migration of stem cells by upregulating SDF-1 expression in astrocytes. For instance, treatment with DETA-NONOate was shown to increase SDF-1 expression in astrocytes and the ischemic brain, which in turn promoted BMSC migration (Cui et al., 2007). Moreover, some inflammatory cytokines, such as tumor necrosis factor-alpha (Blazevski et al., 2015) and IL-1β (Peng et al., 2006), can induce the production of SDF-1 by astrocytes. OSM has also been found to be produced in the context of inflammation, which may be an inducer of SDF-1. In previous studies, OSM was shown to increase breast cancer cell detachment and invasive capacity (Queen et al., 2005) and stimulate SDF-1 expression in human MSCs (Lee et al., 2007). OSM was also shown to induce the activation of STAT3 and ERK pathways in cultured astrocytes (Moidunny et al., 2016), and we indeed found that OSM upregulated SDF-1 expression in astrocytes, resulting in a greater number of migrating BMSCs. Treatment of astrocytes with anti-SDF-1 partially abrogated the OSM-induced migration of BMSCs. Although OSM expression has previously been shown to be induced in inflammatory responses to stimuli, such as lipopolysaccharide (Patel et al., 2013), granulocyte macrophage-colony stimulating factor (Elbjeirami et al., 2011; Pothoven et al., 2017), or PEG2 (Ganesh et al., 2012), little is known regarding the expression of OSM in ischemia reperfusion injury (Zhang et al., 2015; Sun et al., 2015). In vivo, OSM has been shown to be upregulated after spinal cord injury and may promote the functional recovery of mice with spinal cord injury (Slaets et al., 2014). OSM also confers neuroprotection against MCAO stroke (Guo et al., 2015) as well as BMSCs (Zhang and Zhao, 2014). In previous studies, researchers have investigated the additive therapeutic effects of combination treatment with drugs and BMSCs in stroke. For example, combination simvastatin and BMSC treatment upregulates the SDF1/CXCR4 axis, enhances BMSC migration into the ischemic brain, amplifies arteriogenesis and angiogenesis, and improves functional outcomes after stroke (Cui et al., 2009). BMSCs combined with oxiracetam can promote the recovery of neurologic function in MCAO rats, and the effect of combination treatment was better than that with BMSCs alone (Wang et al., 2014). In accordance with these reports, we found that OSM was upregulated in the brains of MCAO rats and that OSM treatment of MCAO rats increased endogenous SDF-1 expression of injured brain. Combination treatment with OSM and BMSCs increased the number of engrafted BMSCs compared with that in the BMSC monotherapy group, and this was significantly correlated with elevated SDF-1 expression to markedly improve functional outcomes in MCAO stroke rats.

Proinflammatory cytokines such as IL-1β and IL-6 are produced mainly by microglia (Shieh et al., 2014) and astrocytes (Nookala and Kumar, 2014), which in turn activate glial cells, inducing further cytokine production and astrogliosis (Zhang et al., 2013). MSCs have been shown to decrease the expression levels of proinflammatory cytokine genes in the context of traumatic brain injury (Drommelschmidt et al., 2017) and stroke (Lv et al., 2017). OSM was shown to decrease the levels of IL-1β (Dumas et al., 2012) but increase levels of IL-6 in astrocytes (Van Wagoner et al., 2000) or human cerebral endothelial cells (Ruprecht et al., 2001), which are not found in BMSCs. Similarly, we demonstrated that combined treatment with OSM and BMSCs significantly decreased the IL-1β expression level but had only a slight effect on IL-6, which may be related to opposing effects of OSM and BMSCs on IL-6 expression. Moreover, combination treatment significantly increased the secretion levels of trophic factors such as VEGF and SDF-1. Thus, we speculate that the detailed mechanism underlying this protection may partially involve the upregulation of VEGF by OSM in BMSCs, as well as the downregulation of proinflammatory cytokines after combined therapy (Fig. 8). However, the specific involvement of these and other factors (e.g., VEGF, MMP-2, CXCL1, and MCP-1) in this mechanism will need to be explored in future studies.

In conclusion, our study indicates that OSM stimulates BMSCs and astrocytes to produce higher levels of SDF-1, which promotes the migration of BMSCs to injured brain areas, possibly by regulating STAT3 and ERK signaling pathways. Ultimately, the combination of OSM with BMSCs enhanced the efficacy of BMSC-based therapy for MCAO stroke. Taken together, the results of this study demonstrate the importance of examining OSM as a strategy for future drug development. The

administration of OSM combined with BMSCs exhibits dual neuroprotective effects in ischemic stroke, emphasizing the potential translation of OSM combined with BMSCs into clinical therapies for central nervous system injury, such as ischemic stroke and brain trauma.

Author contributions

JH, ZF, and XJ designed the experiments; YX, FL, BL, and TH performed the experiments; ZZ and CS performed data collection and analysis; DS, Q OUYANG, YC, YZ, and YT wrote the manuscript together; HS gave some suggestions about the experiment and the manuscript. XJ revised the manuscript and provided financial support. All authors performed the final approval of the manuscript.

Acknowledgments

This study was supported by grants from the Funds for Key Natural Science Foundation of Guangdong (No. 2016B030230004) and the Educational.

Commission of Guangdong (No. 2013CXZDA008), Key Projects of Health Collaborative Innovation of Guangzhou (No. 201400000003-2) to Prof. Xiaodan Jiang, and the Pearl River S&T Nova Program of Guangzhou (No. 201710010047) to Dr. Haitao Sun.

References

Albiero, M., Poncina, N., Ciciliot, S., Cappellari, R., Menegazzo, L., Ferraro, F., Bolego, C., Cignarella, A., Avogaro, A., Fadini, G.P., 2015. Bone marrow macrophages contribute to diabetic stem cell mobilopathy by producing oncostatin M. Diabetes 64, 2957–2968.

Ankrum, J., Karp, J.M., 2010. Mesenchymal stem cell therapy: two steps forward, one step back. Trends Mol. Med. 16, 203–209.

Baker, B.J., Qin, H., Benveniste, E.N., 2008. Molecular basis of oncostatin M-induced SOCS-3 expression in astrocytes. Glia 56, 1250–1262.

Beatus, P., Jhaveri, D.J., Walker, T.L., Lucas, P.G., Rietze, R.L., Cooper, H.M., Morikawa, Y., Bartlett, P.F., 2011. Oncostatin M regulates neural precursor activity in the adult brain. Dev. Neurobiol. 71, 619–633.

Blazevski, J., Petkovic, F., Momcilovic, M., Jevtic, B., Mostarica, S.M., Miljkovic, D., 2015. Tumor necrosis factor stimulates expression of CXCL12 in astrocytes. Immunobiology 220, 845–850.

Boutin, H., Lefeuvre, R.A., Horai, R., Asano, M., Iwakura, Y., Rothwell, N.J., 2001. Role of IL-1alpha and IL-1beta in ischemic brain damage. J. Neurosci. 21, 5528–5534.

Caplan, A.I., Correa, D., 2011. The MSC: an injury drugstore. Cell Stem Cell 9, 11–15.

Caplan, A.I., Dennis, J.E., 2006. Mesenchymal stem cells as trophic mediators. J. Cell. Biochem. 98, 1076–1084.

Chen, S.H., Benveniste, E.N., 2004. Oncostatin M: a pleiotropic cytokine in the central nervous system. Cytokine Growth Factor Rev. 15, 379–391.

Cui, X., Chen, J., Zacharek, A., Li, Y., Roberts, C., Kapke, A., Savant-Bhonsale, S., Chopp, M., 2007. Nitric oxide donor upregulation of stromal cell-derived factor-1/chemokine (CXC motif) receptor 4 enhances bone marrow stromal cell migration into ischemic brain after stroke. Stem Cells 25, 2777–2785.

Cui, X., Chopp, M., Zacharek, A., Roberts, C., Lu, M., Savant-Bhonsale, S., Chen, J., 2009. Chemokine, vascular and therapeutic effects of combination Simvastatin and BMSC treatment of stroke. Neurobiol. Dis. 36, 35–41.

Drommelschmidt, K., Serdar, M., Bendix, I., Herz, J., Bertling, F., Prager, S., Keller, M., Ludwig, A.K., Duhan, V., Radtke, S., de Miroschedji, K., Horn, P.A., van de Looij, Y., Giebel, B., Felderhoff-Muser, U., 2017. Mesenchymal stem cell-derived extracellular vesicles ameliorate inflammation-induced preterm brain injury. Brain Behav. Immun. 60, 220–232.

Dumas, A., Lagarde, S., Laflamme, C., Pouliot, M., 2012. Oncostatin M decreases interleukin-1 beta secretion by human synovial fibroblasts and attenuates an acute inflammatory reaction in vivo. J. Cell. Mol. Med. 16, 1274–1285.

Elbjeirami, W.M., Donnachie, E.M., Burns, A.R., Smith, C.W., 2011. Endothelium-derived GM-CSF influences expression of oncostatin M. Am. J. Phys. Cell Phys. 301, C947–C953.

Franco, E.C., Cardoso, M.M., Gouveia, A., Pereira, A., Gomes-Leal, W., 2012. Modulation of microglial activation enhances neuroprotection and functional recovery derived from bone marrow mononuclear cell transplantation after cortical ischemia. Neurosci. Res. 73, 122–132.

Ganesh, K., Das, A., Dickerson, R., Khanna, S., Parinandi, N.L., Gordillo, G.M., Sen, C.K., Roy, S., 2012. Prostaglandin E(2) induces oncostatin M expression in human chronic wound macrophages through Axl receptor tyrosine kinase pathway. J. Immunol. 189, 2563–2573.

Glezer, I., Rivest, S., 2010. Oncostatin M is a novel glucocorticoid-dependent neuroinflammatory factor that enhances oligodendrocyte precursor cell activity in demyelinated sites. Brain Behav. Immun. 24, 695–704.

Greenberg, D.A., Jin, K., 2013. Vascular endothelial growth factors (VEGFs) and stroke. Cell. Mol. Life Sci. 70, 1753–1761.

Guo, S., Li, Z.Z., Gong, J., Xiang, M., Zhang, P., Zhao, G.N., Li, M., Zheng, A., Zhu, X., Lei, H., Minoru, T., Li, H., 2015. Oncostatin M confers neuroprotection against ischemic stroke. J. Neurosci. 35, 12047–12062.

Hayakawa, K., Esposito, E., Wang, X., Terasaki, Y., Liu, Y., Xing, C., Ji, X., Lo, E.H., 2016. Transfer of mitochondria from astrocytes to neurons after stroke. Nature 535, 551–555.

Hoggatt, J., Singh, P., Sampath, J., Pelus, L.M., 2009. Prostaglandin E2 enhances hematopoietic stem cell homing, survival, and proliferation. Blood 113, 5444–5455.

Huang, C., Zhao, L., Gu, J., Nie, D., Chen, Y., Zuo, H., Huan, W., Shi, J., Chen, J., Shi, W., 2016. The migration and differentiation of hUC-MSCs(CXCR4/GFP) encapsulated in BDNF/chitosan scaffolds for brain tissue engineering. Biomed. Mater. 11, 035004.

Imitola, J., Raddassi, K., Park, K.I., Mueller, F.J., Nieto, M., Teng, Y.D., Frenkel, D., Li, J., Sidman, R.L., Walsh, C.A., Snyder, E.Y., Khoury, S.J., 2004. Directed migration of neural stem cells to sites of CNS injury by the stromal cell-derived factor 1alpha/CXC chemokine receptor 4 pathway. Proc. Natl. Acad. Sci. U. S. A. 101, 18117–18122.

Islam, M.N., Das, S.R., Emin, M.T., Wei, M., Sun, L., Westphalen, K., Rowlands, D.J., Quadri, S.K., Bhattacharya, S., Bhattacharya, J., 2012. Mitochondrial transfer from bone-marrow-derived stromal cells to pulmonary alveoli protects against acute lung injury. Nat. Med. 18, 759–765.

Janssens, K., Maheshwari, A., Van den Haute, C., Baekelandt, V., Stinissen, P., Hendriks, J.J., Slaets, H., Hellings, N., 2015. Oncostatin M protects against demyelination by inducing a protective microglial phenotype. Glia 63, 1729–1737.

Jin, R., Liu, L., Zhang, S., Nanda, A., Li, G., 2013. Role of inflammation and its mediators in acute ischemic stroke. J. Cardiovasc. Transl. Res. 6, 834–851.

Keimpema, E., Fokkens, M.R., Nagy, Z., Agoston, V., Luiten, P.G., Nyakas, C., Boddeke, H.W., Copray, J.C., 2009. Early transient presence of implanted bone marrow stem cells reduces lesion size after cerebral ischaemia in adult rats. Neuropathol. Appl. Neurobiol. 35, 89–102.

Lan, Y.W., Theng, S.M., Huang, T.T., Choo, K.B., Chen, C.M., Kuo, H.P., Chong, K.Y., 2017. Oncostatin M-preconditioned mesenchymal stem cells alleviate bleomycin-induced pulmonary fibrosis through paracrine effects of the hepatocyte growth factor. Stem Cells Transl. Med. 6, 1006–1017.

Lee, M.J., Song, H.Y., Kim, M.R., Sung, S.M., Jung, J.S., Kim, J.H., 2007. Oncostatin M stimulates expression of stromal-derived factor-1 in human mesenchymal stem cells. Int. J. Biochem. Cell Biol. 39, 650–659.

Luo, X., Tai, W.L., Sun, L., Pan, Z., Xia, Z., Chung, S.K., Cheung, C.W., 2016. Crosstalk between astrocytic CXCL12 and microglial CXCR4 contributes to the development of neuropathic pain. Mol. Pain 12.

Lv, B., Li, F., Fang, J., Xu, L., Sun, C., Han, J., Hua, T., Zhang, Z., Feng, Z., Wang, Q., Jiang, X., 2016. Activated microglia induce bone marrow mesenchymal stem cells to produce glial cell-derived neurotrophic factor and protect neurons against oxygen-glucose deprivation injury. Front. Cell. Neurosci. 10, 283.

Lv, B., Li, F., Han, J., Fang, J., Xu, L., Sun, C., Hua, T., Zhang, Z., Feng, Z., Jiang, X., 2017. Hif-1alpha overexpression improves transplanted bone mesenchymal stem cells survival in rat MCAO stroke model. Front. Mol. Neurosci. (10), 80.

Moidunny, S., Matos, M., Wesseling, E., Banerjee, S., Volsky, D.J., Cunha, R.A., Agostinho, P., Boddeke, H.W., Roy, S., 2016. Oncostatin M promotes excitotoxicity by inhibiting glutamate uptake in astrocytes: implications in HIV-associated neurotoxicity. J. Neuroinflammation 13, 144.

Nookala, A.R., Kumar, A., 2014. Molecular mechanisms involved in HIV-1 Tat-mediated induction of IL-6 and IL-8 in astrocytes. J. Neuroinflammation 11, 214.

Patel, O.V., Wilson, W.B., Qin, Z., 2013. Production of LPS-induced inflammatory mediators in murine peritoneal macrophages: neocuproine as a broad inhibitor and ATP7A as a selective regulator. Biometals 26, 415–425.

Peng, H., Erdmann, N., Whitney, N., Dou, H., Gorantla, S., Gendelman, H.E., Ghorpade, A., Zheng, J., 2006. HIV-1-infected and/or immune activated macrophages regulate astrocyte SDF-1 production through IL-1beta. Glia 54, 619–629.

Piao, J.M., Wu, W., Yang, Z.X., Li, Y.Z., Luo, Q., Yu, J.L., 2018. MicroRNA-381 favors repair of nerve injury through regulation of the SDF-1/CXCR4 signaling pathway via LRRC4 in acute cerebral ischemia after cerebral lymphatic blockage. Cell. Physiol. Biochem. 46, 890–906.

Pothoven, K.L., Norton, J.E., Suh, L.A., Carter, R.G., Harris, K.E., Biyasheva, A., Welch, K., Shintani-Smith, S., Conley, D.B., Liu, M.C., Kato, A., Avila, P.C., Hamid, Q., Grammer, L.R., Peters, A.T., Kern, R.C., Tan, B.K., Schleimer, R.P., 2017. Neutrophils are a major source of the epithelial barrier disrupting cytokine Oncostatin M in mucosal airways disease. J. Allergy Clin. Immunol. 139, 1966–1978.e9.

Queen, M.M., Ryan, R.E., Holzer, R.G., Keller-Peck, C.R., Jorcyk, C.L., 2005. Breast cancer cells stimulate neutrophils to produce oncostatin M: potential implications for tumor progression. Cancer Res. 65, 8896–8904.

Ruprecht, K., Kuhlmann, T., Seif, F., Hummel, V., Kruse, N., Bruck, W., Rieckmann, P., 2001. Effects of oncostatin M on human cerebral endothelial cells and expression in inflammatory brain lesions. J. Neuropathol. Exp. Neurol. 60, 1087–1098.

Shi, W., Huang, C.J., Xu, X.D., Jin, G.H., Huang, R.Q., Huang, J.F., Chen, Y.N., Ju, S.Q., Wang, Y., Shi, Y.W., Qin, J.B., Zhang, Y.Q., Liu, Q.Q., Wang, X.B., Zhang, X.H., Chen, J., 2016. Transplantation of RADA16-BDNF peptide scaffold with human umbilical cord mesenchymal stem cells forced with CXCR4 and activated astrocytes for repair of traumatic brain injury. Acta Biomater. 45, 247–261.

Shieh, C.H., Heinrich, A., Serchov, T., van Calker, D., Biber, K., 2014. P2X7-dependent, but differentially regulated release of IL-6, CCL2, and TNF-alpha in cultured mouse microglia. Glia 62, 592–607.

Slaets, H., Nelissen, S., Janssens, K., Vidal, P.M., Lemmens, E., Stinissen, P., Hendrix, S., Hellings, N., 2014. Oncostatin M reduces lesion size and promotes functional recovery and neurite outgrowth after spinal cord injury. Mol. Neurobiol. 50, 1142–1151.

Sohni, A., Verfaillie, C.M., 2013. Mesenchymal stem cells migration homing and tracking. Stem Cells Int. 2013, 130763.

Sun, D., Li, S., Wu, H., Zhang, M., Zhang, X., Wei, L., Qin, X., Gao, E., 2015. Oncostatin M (OSM) protects against cardiac ischaemia/reperfusion injury in diabetic mice by regulating apoptosis, mitochondrial biogenesis and insulin sensitivity. J. Cell. Mol. Med. 19, 1296–1307.

Tang, G., Liu, Y., Zhang, Z., Lu, Y., Wang, Y., Huang, J., Li, Y., Chen, X., Gu, X., Wang, Y., Yang, G.Y., 2014. Mesenchymal stem cells maintain blood-brain barrier integrity by inhibiting aquaporin-4 upregulation after cerebral ischemia. Stem Cells 32, 3150–3162.

Tsai, L.K., Wang, Z., Munasinghe, J., Leng, Y., Leeds, P., Chuang, D.M., 2011. Mesenchymal stem cells primed with valproate and lithium robustly migrate to infarcted regions and facilitate recovery in a stroke model. Stroke 42, 2932–2939.

Van Wagoner, N.J., Choi, C., Repovic, P., Benveniste, E.N., 2000. Oncostatin M regulation of interleukin-6 expression in astrocytes: biphasic regulation involving the mitogen-activated protein kinases ERK1/2 and p38. J. Neurochem. 75, 563–575.

Wang, Y., Deng, Y., Zhou, G.Q., 2008. SDF-1alpha/CXCR4-mediated migration of systemically transplanted bone marrow stromal cells towards ischemic brain lesion in a rat model. Brain Res. 1195, 104–112.

Wang, C., Li, F., Guan, Y., Zhu, L., Fei, Y., Zhang, J., Pan, Y., 2014. Bone marrow stromal cells combined with oxiracetam influences the expression of B-cell lymphoma 2 in rats with ischemic stroke. J. Stroke Cerebrovasc. Dis. 23, 2591–2597.

Yamasaki, Y., Matsuura, N., Shozuhara, H., Onodera, H., Itoyama, Y., Kogure, K., 1995. Interleukin-1 as a pathogenetic mediator of ischemic brain damage in rats. Stroke 26, 676–680 (discussion 681).

Yang, G.Y., Betz, A.L., Hoff, J.T., 1994. The Effects of Blood or Plasma Clot on Brain Edema in the Rat with Intracerebral Hemorrhage: Acta Neurochir Suppl (Wien). 60. pp. 555–557.

Yang, C., Zhou, L., Gao, X., Chen, B., Tu, J., Sun, H., Liu, X., He, J., Liu, J., Yuan, Q., 2011. Neuroprotective effects of bone marrow stem cells overexpressing glial cell line-derived neurotrophic factor on rats with intracerebral hemorrhage and neurons exposed to hypoxia/reoxygenation. Neurosurgery 68, 691–704.

Zhang, Q., Zhao, Y.H., 2014. Therapeutic angiogenesis after ischemic stroke: Chinese medicines, bone marrow stromal cells (BMSCs) and their combinational treatment. Am. J. Chin. Med. 42, 61–77.

Zhang, R., Liu, Y., Yan, K., Chen, L., Chen, X.R., Li, P., Chen, F.F., Jiang, X.D., 2013. Anti-inflammatory and immunomodulatory mechanisms of mesenchymal stem cell transplantation in experimental traumatic brain injury. J. Neuroinflammation (10), 106.

Zhang, M., Wang, C., Hu, J., Lin, J., Zhao, Z., Shen, M., Gao, H., Li, N., Liu, M., Zheng, P., Qiu, C., Gao, E., Wang, H., Sun, D., 2015. Notch3/Akt signaling contributes to OSM-induced protection against cardiac ischemia/reperfusion injury. Apoptosis 20, 1150–1163.